Hindawi
Wireless Communications and Mobile Computing
Volume 2022, Article ID 7476157, 16 pages
https://doi.org/10.1155/2022/7476157

Research Article

Performance Analysis of Distance-Based D2D Matching Mechanism

Qiaoshou Liu, Yingchen Gu, Jiaxin Wang, and Jianwen Zou

School of Communication and Information Engineering, Advanced Network and Intelligent Connection Technology Key Laboratory of Chongqing Education Commission of China, Chongqing Key Laboratory of Ubiquitous Sensing and Networking, Chongqing University of Posts and Telecommunications, Chongqing 400065, China

Correspondence should be addressed to Yingchen Gu; 378180329@qq.com

Received 9 June 2022; Accepted 1 August 2022; Published 16 August 2022

Academic Editor: Quoc-Tuan Vien

The traditional cellular architecture where devices connect to their service base station (BS) may cause poor performance especially for edge users. Device-to-device (D2D) communication enables nearby user as a relay to help BS forward information, thereby improving the network coverage and quality of service (QoS) of edge users. This paper proposes a distance-based D2D matching mechanism for general cellular networks, where a relay user who successfully connects to its targeted BS can transmit data to its closest user for D2D communication. A link of BS to D2D pair contains two sublinks, which occur at different time phases in each cell. Assuming a nonsynchronous system, we consider that there exists cross-layer interference for D2D links. Based on the techniques of stochastic geometry, we develop the performance of coverage probability and ergodic rate of the D2D network. A key intermediate step in this analysis is the derivation of the interference expressions for D2D links caused by BSs and cochannel D2D users. Then, we derive the meta distribution of the signal-to-interference ratio (SIR) to capture the performance changes of individual links. Simulation results demonstrate that our matching mechanism based on the appropriate time resource allocation favors the edge users with a higher probability of successful communication and transmission rate.

1. Introduction

1.1. Motivation. In recent years, the availability of Internet of things (IoT) devices has a tremendous growth, which is nearly 22 billion (by 2020) and would go up to 30 billion approximately by the end of 2025 [1]. Due to the rapid increase in the number of connected devices, effective wireless spectrum management has become a top priority. In this regard, D2D communication has been a critical research direction. D2D communication is one of the evolving technologies of the fifth generation of mobile communication (5G) networks, providing opportunities for proximity-based services [2]. This technology helps the BS counterbalance the network load by using underlay or overlay modes. In underlay mode, both the cellular users (CUs) and D2D users (DUs) use the same spectrum resources, which can provide higher spectrum efficiency at the expense of communication quality due to the extra interference. While in overlay mode, the system can provide a dedicated spectrum resource for D2D pairs so there is no interference between DUs and CUs [3]. Furthermore, D2D communication improves the quality of service (QoS), quality of experience (QoE), and proximity gain for the network users [4]. It allows a user as a relay to assist a source in communicating to its destination, so the successful communication probability would be improved among edge users with the shorter communication distance.

At present, the main research contents of D2D communication mainly involve resource management, D2D relay selection, and interference control. In [5], a robust distributed resource allocation solution was proposed, which can maximize the network sum rate when the interference from other relay nodes and the link gains are uncertain. In [6], a centralized signaling algorithm was proposed to exchange D2D discovery messages. The authors of [7–9] adopted fractional frequency reuse (FFR) technology to reduce the

cochannel interference between cellular and D2D links, enabling to maximize the system throughput. In [7], Jain's fairness index method was introduced to guarantee fairness of resources allocation between CUs and DUs. A greedy heuristic search algorithm and binary power control scheme were proposed to improve the throughput of D2D system [8]. In [9], an optimization problem based on Lagrange relaxation technique and combinatorial auction matching algorithm was proposed to solve data traffic and guarantee the QoS of CUs and DUs. In [10], a new multilevel over-the-air aggregation scheme for a wireless multihop D2D-based mobile edge computing system was proposed, which aimed to reduce the communication resource overhead. The authors of [11] focus on the spectrum access problem for D2D-assisted cellular networks, designing a generalized double deep Q-network algorithm to maximize the sum throughput. The D2D relaying mechanism consists of two time phases [12]: the discovery phase and the data transmission phase. While in the discovery phase, a relay user seeks and selects a receiver for D2D communication, then the relay transmits data to its receiver in the data transmission phase. For downlink cellular links, D2D discovery phase is the process of BSs selecting the relays. The relay selection can be performed in a centralized manner [13, 14] or distributed manner [15, 16]. With the centralized approach, the BS selects the relay user, whereas with the distributed approach, it is the user itself that selects the relay and communicates with it. The above literature studied the allocation scheme of spectrum resources in data transmission phase and made a great contribution to the spectrum allocation of D2D networks, but most of them ignore the discovery phase of D2D systems and therefore do not consider the time resources distribution in terms of the D2D discovery phase and data phase.

To evaluate the benefits of introducing D2D technology to the cellular network, a comprehensive analysis of the network needs to be performed. Stochastic geometry is a popular mathematical tool for modeling and analyzing D2D networks recently [17–19]. Coverage probability and ergodic rate, as two fundamental performance metrics, are derived by the spatial average of some point processes, especially by the Poisson point process (PPP). The coverage probability mainly answers the limited information "For a certain SIR threshold, how many mobile users on average can successfully access to the network?". The authors of [5, 6, 11] analyzed spatial average of D2D relay networks such as coverage probability; however, there is little work to study the more fine-grained performance index of D2D relay networks, which is a key performance metric in wireless networks, i.e., the meta distribution of the SIR. The meta distribution concentrates more detailed information on what fraction of users whose network access success probability is greater than a given value [20] across the entire network. The meta distribution is first introduced in Poisson bipolar networks, which expressions were exactly and approximately derived [20]. The authors of [21] focus on the meta distribution of the SIR for the cache-enabled networks with the application of random caching and random discontinuous transmission schemes. In [22], the authors focus on the analysis of the meta distribution of the SIR for the ultradense network (UDN) with directional antenna. And the moments of the meta distribution for which scenery are obtained. In [23], a mathematical framework for meta distribution of cell-center users and cell-edge users was proposed, which is aimed to capture the spatial (geographical location) and temporal randomness (queue status) of cellular traffic by using queueing theory and stochastic geometry. The mean local delay is in itself an important performance indicator, which shows the mean number of transmission attempts for a node to successfully transmit a packet to its target receiver [24]. Hence, it is critical to further investigate how the D2D relaying scheme affect the performance of individual links. This is accomplished through fine-grained performance indicators that can straight capture individual users' performance for D2D network with appropriate matching mechanism.

1.2. Related Work. A number of outstanding works have contributed to the D2D networks based on stochastic geometry. A new spatial model to study the performance of coverage probability for D2D networks was developed in [25], where D2D users (DUs) locations are modeled as a Poisson cluster process (PHP). In [26], an analytical framework for a cellular network with underlying D2D communications was proposed, which was based on a probabilistic distance and path loss model. In [27], the authors combined a channel allocation policy with three power control schemes to mitigate interference in a D2D underlaid cellular network, which was modeled as a random network based on stochastic geometry. The authors of [28] analyzed the coverage of cyclic prefix OFDM-based D2D cellular networks using stochastic geometry. Two D2D transmission policies were designed in [29] for D2D transmitter (DT) energy harvest from cellular systems. In scheme 1, D2D communication can be established only when meeting the energy constraint. In scheme 2, the guard zone is considered to avoid interference and is modeled by the Poisson hole process (PHP) to analyze the main performance indicators. In [30], a new interference management approach for D2D cellular networks was presented, which required selecting the optimum mode between half-duplex and in-band full-duplex to maximize the D2D throughput and guarantee the delay of cellular users (CUs). The authors of [31] studied the ergodic rate and average service delay for user terminals in the clustered cache-enabled small cell networks and mmWave D2D networks with stochastic geometry method. Furthermore, the analysis of throughput and AoI performance metrics using this method in an IoT network was presented [32], where the throughput was characterized when the IoT devices were in D2D mode and the latter was considered in cellular fashion. In [33], a distributed relay selection scheme was proposed to reduce the total energy consumption for massive machine-type communications (mMTC) devices, which was to use a contention process based on a truncated geometric distribution.

The contributions of the above-mentioned literature have to be acknowledged, for the exact expressions of main performance indicators are all derived based on their

proposed D2D network models. However, most of them make the assumption of a fixed D2D link distance for the convenience of analyzing the network performance, which is quite limiting because it is relaxed by assuming that the expected D2D receiver (DR) is uniformly distributed within a circle around the DT it serves. This restriction is more appropriate for an ad hoc network scenario. In actual deployment, users tend to prefer to access closer transmission sources to communication from a statistical point of view. Different from the above-mentioned references, we introduce a novel distance-based user division and D2D matching policy in the cellular network and derive the mathematical analytical expressions including coverage probability and meta distribution through stochastic geometry, which can better describe the D2D network characteristics.

1.3. Contributions and Outcomes. In this paper, the D2D technology with distance-based relaying scheme is introduced in the general downlink one-tier cellular network. We mainly explore that the effect of different time resource allocation in this scheme on the network performance. The main contributions of this work are summarized as follows.

(1) We develop a novel user partitioning and D2D matching mechanism, which is based on the distance to their serving BSs. In particular, CUs within the disk of D around the BS are directly targeted with the BS to avoid more energy consumption, whereas the rest of DUs who are closer to the serving BS have priority to become relay users in the first time phase and forward data to the more marginal users in the next phase for D2D communication. The BS first selects the nearest DU as DT, and the DT in the second phase looks for the nearest user as the DR under the control of their BS. Then, the BS ignores the pairs that have successfully communicated in the subsequent relaying process until all DUs have been paired

(2) Since different time slots have different transmission sources, we model a nonsynchronization system in which the BS-D2D pairs of each cell can occur at different time instants. This favors that the network has lower signaling overhead. For this setup, DUs will be interfered by BSs (except the serving BS) with some probability. To mitigate interference between D2D and cellular communications, we assume overlay in-band D2D, so DUs can be approximatively modeled as a Poisson hole process

(3) Based on the stochastic geometry tool, we derive the coverage probability and ergodic rate of CUs, DUs, and the whole network under the proposed D2D network above. And time resource allocation for D2D links is taken into consideration. Furthermore, a much sharper version provided by meta distribution of SIR is obtained. And some performance indicators like the variance of standard coverage probability and the mean local delay can be obtained to evaluate the individual link information

(4) The analysis leads to several useful design insights. It reveals that more time consumed by BS-DT links has a same effect on the BS-DT links and DT-DR links for coverage and transmission rate; i.e., both of these two performance indicators will be improved for these links. Thus, the number of users who can successfully access the network also has increased. This observation shows that more DTs successfully communicate in the first time stage, and consequently in the second stage, there exist more successful D2D links

The rest of the paper is organized as follows. Section 2 presents the system model considered in this paper. In Section 3, we present our D2D relaying mechanism. In Section 4, the main results of coverage probability, ergodic rate, and the meta distribution of SIR are derived. The numerical results and discussion are presented in Section 5. Finally, conclusions and extensions of future work are given in Section 6.

2. System Model

We consider a downlink cellular network, where all users and BSs form two independent homogeneous Poisson point processes (HPPPs) Φ_u and Φ_b with densities λ_u and λ_b, respectively. All BSs directionally transmit messages to users by beamforming, whereas all users are equipped with isotropic antennas. The specific process of beamforming is beyond the scope of this article. All BSs are equipped with massive MIMO and directionally transmit messages to users by beamforming, whereas all users are equipped with single isotropic antennas. In this paper, we do not consider the specific process of beamforming. As shown in Figure 1, we assume that users within the disk of predefined radius D, called internal CUs, can be directly accessed to their closest BSs in Euclidean distance (cellular mode), while the rest of the users outside the disk can start D2D communication (D2D mode). We call the area outside the predefined radius D around BS as the D2D area. For example, a user in the D2D area with poor coverage may use a nearby user as a relay to enhance the cellular capacity and network coverage. In our model, we consider that BSs are the central management system to exchange required signaling messages for D2D communication so the relay users can only forward messages from the BSs, not act as BSs. Since different time slots have different transmission sources, we assume that the transmission of BS-DT-DR links in each cell for the entire network is not synchronous in terms of time resources. This assumption reduces the additional signaling overhead compared to synchronization. When the transmission is nonsynchronous, DUs are interfered by all other BSs except service BS with a probability of less than 1. While in the case of synchronous transmission, D2D suffers the serious interference with a probability of 1, which also explains the rationality of our model. The frame structure of synchronous transmission and asynchronous transmission is shown in Figure 2. The main notations used in this paper are summarized in Table 1.

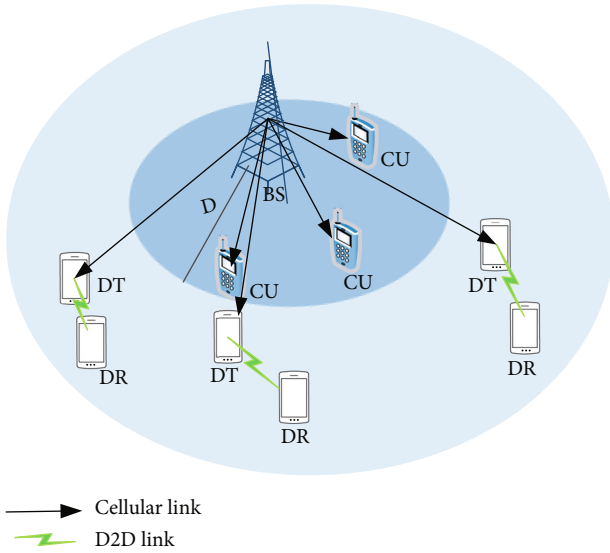

Figure 1: Network model: CUs within the disk of predefined radius D directly access to their target BS, whereas users outside the disk of D (D2D area) can establish D2D communication under the control of the BS. For BS-D2D links, BS chooses a nearest user as a relay (DT) in the first stage and this relay transmit to a nearest DR in the second stage.

2.1. Time-Frequency Allocation Policy. In the BS-D2D link, the transmission process is divided into two phases and the time consumed by the two phases are t_1 and t_2. In the first stage, a BS sends messages to a potential relay user (DT). In the second stage, when the potential DT has successfully established with its serving BS, it starts to forward the information to its nearest user (DR) in the D2D area for establishing D2D communication. To maximize the utilization of spectrum resources, all BSs reuse all spectrum resources. The spectrum resources are evenly divided into M orthogonal channels, where the set of channels $\mathcal{N} = \{n_1, n_2, \cdots, n_{|\mathcal{N}|}\}$ for data transmission in cellular links, with $|\mathcal{N}|$ denoting the number of channels. The rest set of channels $\mathcal{K} = \{k_1, k_2, \cdots, k_{|\mathcal{K}|}\}$ is reserved for data transmissions of D2D links, $|\mathcal{N}| + |\mathcal{K}| = M$. The mobile users are assumed to operate in half-duplex mode, so they only transmit and receive data in a channel at different time slots. Therefore, for a D2D link connected to a BS, the downlink traffic is first transmitted over the cellular link and then over the D2D link. Each CU is randomly allocated a channel from $\mathcal{N}$, and each DT-DR link is randomly selected a channel from $\mathcal{K}$ for D2D communication. The total spectrum bandwidth of the system is \textit{BW}, and the set of channels $\mathcal{N}$ and $\mathcal{K}$ occupy f_c and f_d, respectively. We consider the spectrum resources of cellular links and D2D links are equally partitioned in this paper. There are no overlapping channels between f_c and f_d. Thus, D2D pairs (DUs) can be approximatively modeled as PHP with density $\lambda_d = \lambda_u e^{-\lambda_b \pi D^2}$ [34]. We assume the network is fully loaded, which means all BSs are active, and channels are always occupied by associated users. For a BS-CU link, the interference only comes from other BSs except service BSs. While the interference source of DT and DR has two parts, including cochannel interference and cross-tier interference because of the nonsynchronization system model it is worth noting that each cell has at most one same frequency interference DTs. Thus, the interference comes from all BSs except the serving BS, and all cochannel DTs in other BSs except the serving BS for a DT or a DR. We denote the set of cochannel DTs as Φ_{dt} with the same density as the BS λ_b.

2.2. Propagation Model. We model the signal propagation considering large-scale fading and small-scale fading (Rayleigh fading). Generally, Rayleigh fading channel is more suitable for non-line-of-sight link between transmitter and receiver. And it is noteworthy that the cellular network inevitably encounters obstacles such as buildings and trees on the propagation path [35]. In an actual cell, a downlink between a BS and its serving user is independent of other interference cells. Therefore, Rayleigh fading is selected to model multipath fading, which follows an i.i.d. exponential distribution with mean 1, i.e., $h \sim \exp(1)$. The assumption of i.i.d is helpful to derive the Laplace transform of interference. For the large-scale fading, the power loss model with path loss exponent $\alpha > 2$ is adopted [36]. The BSs and the DTs are assumed to keep constant transmit powers of P_b and P_u, respectively. Thus, the received power is obtained as $P_{r_{i,j}} = P_x h_{i,j} r_{i,j}^{-\alpha_{i,j}}$, where P_x is the transmission power of the transmitter i, and the subscript x represents b or u. $r_{i,j}$ is the Euclidean distance between transmitter i and receiver j, and $h_{i,j}$ and $r_{i,j}^{-\alpha_{i,j}}$ are the channel gain factor and pass-loss exponent between transmitter i and receiver j, respectively. To simplify the mathematical analysis, we consider the same path loss parameters (h and α) in all links. However, cellular communications and D2D communications have different path loss parameters in a realistic scenario. For the notational simplicity and mathematical derivations, we focus on a typical random cell, termed representative cell, and analyze the performance of the proposed D2D network. The analysis is performed for a typical user in the representative cell, which is the user chosen uniformly at random among any type users in the network. Without loss of generality, the analysis is performed for the typical user located at the origin o according to the Slivnyak theorem [37]. We denote by b_o the BS which is closest to a typical user.

In addition to the large-scale fading and small-scale fading mentioned above, the angle fading of directional antenna is also considered in this paper [22]. According to the characteristic of directional antenna, only when users are within the range of effective radiation angle of directional antenna Ψ, $\Psi \in (0, 2\pi]$, they can receive the interference or desired signals; otherwise, the links are broken. We assume the angle fading follows the exponential distribution. For the BS-CU link, the SIR at the typical CU is

$$\mathrm{SIR}_c = \frac{P_b h r_c^{-\alpha}}{\sum_{i \in \Phi_b \setminus \{b_o\}} P_b h_i R_i^{-\alpha} e^{-|\theta_i|}}, \quad (1)$$

where R_i denotes the generic random variable for the

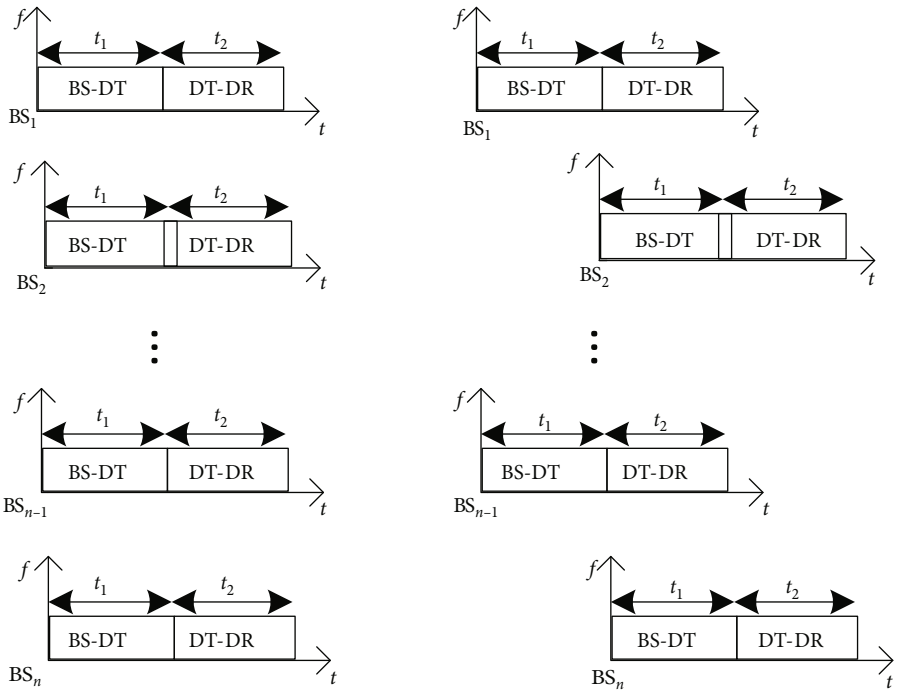

Figure 2: The frame structure of synchronous transmission and asynchronous transmission.

Table 1: Notations.

Notation	Description
$\Phi_b;\lambda_b$	PPP of BSs; intensity of Φ_b
$\Phi_u;\lambda_u$	PPP of users; intensity of Φ_u
$\Phi_{\mathrm{dt}};\lambda_d$	PHP of DUs; intensity of Φ_{dt}
Ψ	Effective radiation angle of directional antennas
P_b	Transmission power of BSs
P_u	Transmission power of users
t	The total time slot
θ	The fading gain of the interference signals for cellular links
α	Path loss exponent for both cellular links and D2D links
h	Rayleigh fading channel with unit mean for both cellular links and D2D links
$\beta;T$	Target SIR of cellular links; target SIR of D2D links
$R_c;R_d$	The serving distance of BS-CU links; the serving distance of BS-DT links
y	The serving distance of DT-DR links

distance between the typical CU and the i^{th} interfering BS, $i \in \Phi_b \setminus \{b_o\}$, and θ_i denotes the value of the angle offset between the location of the typical CU and the antenna boresight directions of its interfering BSs; it is an i.i.d random variable and follows from uniform distribution on $[0, 2\pi]$.

For the BS-DT-DR link, since the asynchronous transmission, the total interference seen at the typical DT originates from two sources: (i) interference caused by BSs (except the serving BS) at the same time slot t_1 is defined as $I_c = (t_1/t_1 + t_2)\sum_{i\in\Phi_b\setminus\{b_o\}} P_b h_i R_i^{-\alpha} e^{-|\theta_i|}$, and (ii) cochannel interference caused by the DT at time slot t_2, which is defined as:$I_d = (t_2/t_1 + t_2)\sum_{i\in\Phi_{\mathrm{dt}}\setminus\{\mathrm{dt}_o\}} P_u h_i Y_i^{-\alpha}$, where Y_i is the distance from cochannel DTs to the typical DT. We let $\mu_i = t_i/t_1 + t_2 (i = 1, 2)$, which is the ratio of BS-CU phases or DT-DR phases to total time, and it is regarded as a constant in the calculation. μ_i also represents the interference probability of BS or cochannel DTs other than serving source for DUs. The SIR of the typical DT is

$$\mathrm{SIR}_{\mathrm{dt}} = \frac{P_b \mathrm{h} r_d^{-\alpha}}{I_c + I_d}, \tag{2}$$

Similarly, the SIR of the typical DR is

$$\mathrm{SIR}_{\mathrm{dr}} = \frac{P_u \mathrm{hy}^{-\alpha}}{I_d + I_c}, \tag{3}$$

where r_c, r_d, and y are the serving distance for cellular links and D2D links, respectively.

3. D2D Relay Pairing Mechanism

3.1. Assumption. Before introducing our relaying mechanism, the following assumptions are made:

(i) Relays have no control on the channel usage and resource allocation. They simply decode and forward received signals to the destinations

(ii) The set of all D2D pairs satisfy the condition $r_{b,d} > D$, where $r_{b,d}$ is the BS-DU distance and D is the distance threshold. In this paper, we predefine D according to the distance from BS to user. In other words, after dividing users, the cellular area is proportional to the D2D area according to the distribution of HPPP. In the PPP-PHP mixed model, the condition $r_{b,d} > D$ is equivalent to considering that users can establish D2D communication if and only if they are located outside a circular area of radius D centered around the BS. This area is called the D2D area

(iii) We assume that a relay receives the desired signal from its tagged BS, part of which is used to ensure its own communication quality, and the rest is used to forward to a DR user in the next time slot. A relay DT can send messages to only one DR. And D2D communication only occurs in the same cell; that is to say, D2D communication fails when they are across the cell

3.2. D2D Relaying Mechanism. We introduce the D2D relaying procedures in a representative cell. These procedures consist of the following steps:

(1) User division policy: The BS measures the BS-user distance r_{bu}. Users in the represent cell can be partitioned into two types based on the relative distance to their tagged BS r_{bu}: CUs and DUs, where DUs include DTs and DRs. Users start the D2D matching phase if and only if $r_{b,d} > D$; otherwise, it communicates directly to the BS. D determines the transmission mode, which avoids unnecessarily using a relay mechanism in each cell, e.g., in case the BS-CU link has very short distance

(2) Pair process: After screening out the CUs, the BS starts searching for the nearest DUs as the first potential relay. Then, the potential relay switches from reception state to transmission state and waits to transmit data received by BS to the rest DUs. Then, the BS measures the distance between DUs r_{uu} and determines whether the number of remaining DUs besides the potential relay is great than 0. Only if the number of remaining DUs is greater than 0, the BS starts allocating the nearest DU for this potential relay as the first DR to establish a D2D link, which is based on r_{uu}. Finally the BS ignores the first D2D link that is already paired and repeats the above steps until there are no DUs left

(3) Data transmission: If the potential DT finds a DR in the rest DUs, it transforms from reception state to transmission state and establishes a D2D link with the selected DR to transmit data. Otherwise, the DT is still a receiver and communicates directly to the BS

4. Analytical Model

In this section, we derive analytical expressions to evaluate our proposed network. First, we focus on the analysis of the total coverage probability and ergodic rate of networks, including the probability that the relay selects a receiver during the matching process and the probability that DRs successfully receive messages from DTs. An intermediate step in our analysis is the deviation of distance distributions from transmitter to receiver. Another indicator that we analyze is the meta distribution. The differences resulting from users in differential network environments lead to unequal communication link quality among users. To evaluate the link-level performance for the whole network, a new performance index, namely, the meta distribution of SIR, was introduced in [20].

4.1. Relevant Distance Distributions. For the BS-CU and BS-DU link, denoting the distances from a typical user to its nearest BS by R_c and R_d, respectively, since the R_c is smaller than D and R_d is greater than D, then, the distribution of R_c conditioned on $R_c < D$ is given by

$$f_{R_c}(r_c|D) = \frac{2\pi\lambda_b r_c e^{-\lambda_b \pi r_c^2}}{1 - e^{-\lambda_b \pi D^2}}, 0 \le r_c \le D, \tag{4}$$

which is a truncated version of the Rayleigh distribution [37].

Proof. The cumulative distribution function (CDF) of R_c conditioned on $R_c < D$

$$\begin{aligned} F_{R_c}(r_c|D) &= \frac{\mathbb{P}\{R_c < r, R_c < D\}}{\{R_c < D\}} = \frac{1 - \mathbb{P}\{R_c \ge r, R_c < D\}}{\mathbb{P}\{R_1 < D\}} \\ &= \frac{1 - e^{-\lambda_b \pi r_c^2} + e^{-\lambda_b \pi D^2}}{1 - e^{-\lambda_b \pi D^2}}. \end{aligned} \tag{5}$$

Taking the derivative of Equation (5), Equation (4) is obtained.

Similarly, the distribution of R_d conditioned on $R_d > D$ is given by

$$f_{R_d}(r_d|D) = \frac{2\pi\lambda_b r_d e^{-\lambda_b \pi r_d^2}}{e^{-\lambda_b \pi D^2}}, r_d > D. \quad (6)$$

For the DT-DR link, we denote the distances from a typical DR to its nearest DT by Y, and the distribution of Y according to the property of PPP is

$$f_Y(y) = 2\pi\lambda_d y e^{-\lambda_d \pi y^2}, \quad (7)$$

where $\lambda_d = \lambda_u e^{-\lambda_b \pi D^2}$ according to reference [37].

4.2. Coverage Probability. The coverage probability can be formally defined as the probability that SIR experienced by a typical user is greater than a desired threshold for successful demodulation and decoding. Mathematically, it is $P_c = \mathbb{E}[\mathbf{1}(\mathrm{SIR} > \beta)] = \mathbb{P}(\mathrm{SIR} > \beta)$, where β is the target SIR threshold of cellular link. We now use the distance distributions presented above subsection to characterize the coverage probability of different types of users.

(1) For the BS-CU link, a typical CU served by the tagged BS b_o is

$$P_c^{\mathrm{cu}} = \frac{\pi - \pi e^{-\lambda_b D^2(\pi + 2F_1(\beta))}}{A_1(\pi + F_1(\beta))}, \quad (8)$$

where $A_1 = 1 - e^{-\lambda_b \pi D^2}$, which is the probability that the user is an CU. Ψ represents the effective radiation angle of directional antenna, which value ranges from 0 to 2π. $F_1(\beta) = \int_1^\infty \int_0^{\Psi/2} (m\beta/(\beta + \beta m^\alpha * e^\theta)) d\theta \mathrm{dm}$.

Proof. See Appendix A.

A typical user DT served by the tagged BS b_o is

$$p_c^{\mathrm{dt}} \geq \frac{2\pi\lambda_b}{A_2} \int_D^\infty r_d e^{-\lambda_b \left(\pi r_d^2 + 2r_d^2 F_2(\beta) + 2\pi e^{-\lambda_b \pi D^2} F_3(T)\right)} \mathrm{dr}_d, \quad (9)$$

where $A_2 = e^{-\lambda_b \pi D^2}$, which is the probability that the user is an DU. $F_2(\beta) = \exp(-2\lambda_b \int_1^\infty \int_0^{\Psi/2} (m\beta/\beta + (1/\mu_1) m^\alpha e^\theta) d\theta dv)$. $F_3(T) = \int_1^\infty (\mathrm{fT}/T + (1/\mu_2)(P_b/P_u) f^\alpha) df$, where T is the SIR threshold of D2D links and X is the distance between interference DTs to the typical DT. We suppose λ_u is large enough, so X is simply considered to be greater than the service distance. The reason for using the greater than or equal sign is that the distance from the DT to the BS is generally smaller than the distance from the DR to the BS, so the received desired signal from BS is larger.

Proof.

$$\begin{aligned} \mathrm{P}_c^{dt} &\geq \int_D^\infty \mathbb{P}(\mathrm{SIR}_{\mathrm{dt}} > \beta | r_d) f_{R_d}(r_d|D) dr_d \\ &= \int_D^\infty \frac{P_b h r^{-\alpha}}{I_c + I_d} f_{R_d}(r_d|D) dr_d = \int_D^\infty \mathscr{L}_{I_{\mathrm{Ic}}}(\beta r_d^\alpha) \mathscr{L}_{I_{\mathrm{Id}}}\left(\frac{T r_d^\alpha}{P_b}\right) f_{R_d}(r_d|D) dr_d, \end{aligned} \quad (10)$$

where $f_{R_d}(r_d|D)$ are given by Equation (5). The proof of $\mathscr{L}_{I_{\mathrm{Ic}}}(\beta r_d^\alpha)$ and $\mathscr{L}_{I_{\mathrm{Id}}}(T r_d^\alpha / P_b)$ is the same as the typical CU, but the user is equipped with an isotropic antenna, so there is no angular fading in D2D link and $\mathscr{L}_{I_{\mathrm{Id}}}(T r_d^\alpha / P_b)$ is one less layer of integration.

(2) The DT can forward data to the DR in time slot 2 only after it successfully connects to the BS in time slot 1, so a typical DR served by the tagged DT_o is

$$\mathrm{P}_c^{\mathrm{dr}} \geq \frac{8\pi^3 \lambda_d \lambda_b^2}{A_2^2} \int_0^\infty \int_D^\infty r_d^2 y e^{-\lambda_b \left(2\pi r_d^2 + 2F_4(r_d,\beta) + 2\pi y^2 e^{-\lambda_b \pi D^2} F_5(T) + 2r_d^2 F_2(\beta) 2\pi e^{-\lambda_b \pi D^2} F_3(T)\right)} e^{-\lambda_d \pi y^2} \mathrm{dr}_d \mathrm{dy}, \quad (11)$$

where F_2 function and F_3 function are the same as above. $F_4(r_d, \beta) = \int_{r_d}^\infty \int_0^{\Psi/2} (v\beta/\beta + (1/\mu_1)(P_u/P_b)(v/y)^\alpha e^\theta) d\theta \mathrm{dv}$ and $F_5(T) = \int_0^\infty (gT/T + (1/\mu_2) g^\alpha) \mathrm{dg}$.

Proof. See Appendix B.

Theorem 1. *The total coverage probability of the network is*

$$P_c^{total} = A_1 P_c^{cu} + A_2 P_c^{dt} + A_2 P_c^{dr}, \quad (12)$$

where P_c^{cu}, P_c^{dt}, and P_c^{dr} are given by Equations (8), (9), and (11), respectively.

4.3. Ergodic Transmission Rate of D2D Network. The ergodic rate of users is given by [36], i.e., $\mathbb{E}[\ln(1 + \mathrm{SIR})]$. Exploiting the fact that $\ln(1 + \mathrm{SIR})$ is a monotonically increasing function of SIR, we arrive at

$$\tau = \int_{t>0} P\left[\mathrm{SIR} > 2^t - 1\right] \mathrm{dt}. \quad (13)$$

Thus, the average rate is equivalent to the coverage probability evaluated at $\beta = 2^b - 1$ or $T = 2^t - 1$ and then integrated over b or t. The coverage of a typical cellular link or a D2D link is given by Equations (8), (9), and (11). Thus, the average rate of the BS-CU link can be obtained by substituting $\beta = 2^b - 1$ into Equation (8), and integrating the result over b, the final expression is given by

$$\tau^{\mathrm{cu}} = \int_0^\infty \frac{\pi - \pi e^{-\lambda_b D^2 \left(\pi + 2F_1\left(2^b - 1\right)\right)}}{A_1\left(\pi + F_1\left(2^b - 1\right)\right)} \mathrm{db}. \quad (14)$$

Table 2: Simulation parameters.

Parameter	Value
Intensity of BSs λ_b	$2 * 10^{-5}$
Intensity of users λ_u	$8 * 10^{-4}$
Effective radiation angle of directional antennas Ψ	$\pi/2$
Transmission power of BSs P_b	33 dBm
Transmission power of users P_u	27 dBm
Total simulated area S	1000m * 1000m
Distance division threshold D	72.8m
Pass-loss exponent α	4
Spectrum bandwidth B	180 KHz

Similarly, the average rate of the BS-DT link and DT-DR link can be obtained by substituting $\beta = 2^b - 1$ and $T = 2^t - 1$ into Equations (9) and (11), and integrating the result over b and t, the final expressions are given by Equations (15) and (16), respectively.

$$\tau^{\mathrm{dt}} \geq \frac{2\pi\lambda_b}{A_2}\int_0^{\infty}\int_0^{\infty}\int_D^{\infty} r_d e^{-\lambda_b\left(\pi r_d^2+2r_d^2F_2\left(2^b-1\right)+2\pi e^{-\lambda_b\pi D^2}F_3\left(2^t-1\right)\right)}\mathrm{d}r_d\mathrm{d}t\mathrm{d}b, \tag{15}$$

$$\tau^{\mathrm{dr}} \geq \frac{8\pi^3\lambda_b^2\lambda_d}{A_2^2}\int_0^{\infty}\int_0^{\infty}\int_0^{\infty}\int_D^{\infty} r_d^2 y e^{-\lambda_b\left(2\pi r_d^2+2F_4\left(r_d,2^b-1\right)+2\pi y^2 e^{-\lambda_b\pi D^2}F_5\left(2^t-1\right)+2r_d^2F_2\left(2^b-1\right)2\pi e^{-\lambda_b\pi D^2}F_3\left(2^t-1\right)\right)}e^{-\lambda_d\pi y^2}\mathrm{d}r_d\mathrm{d}y\mathrm{d}b\mathrm{d}t. \tag{16}$$

For the BS-DT-DR link, the link is divided into two sublinks. Only when the SIR received by the two sublinks are greater than the specified threshold, data can be successfully communicated through the link. So the transmission rate of the BS-DT-DR link depends on the smaller value between τ^{dt} and τ^{dr}, i.e.,

$$\tau^{\mathrm{du}} = \min\left\{\tau^{\mathrm{dt}}, \tau^{\mathrm{dr}}\right\}. \tag{17}$$

Theorem 2. *For the overall users, the ergodic rate is*

$$\tau_c^{total} = A_1\tau^{cu} + A_2\tau^{du}, \tag{18}$$

where the τ^{cu} and τ^{du} are given by Equations (14) and (17), respectively.

4.4. The Meta Distribution of D2D Network. The meta distribution $\bar{F}_{P_s}(x)$ is the complementary cumulative distribution function (CCDF) of the random variable

$$P_s(\beta) \triangleq \mathbb{P}(\mathrm{SIR}_0 > \beta|\Phi), \tag{19}$$

which is the CCDF of the conditional SIR of the typical user given the points processes and conditioned on the desired transmitter to be active. Hence, the meta distribution is formally given by [20]:

$$\bar{F}_{P_s}(x) \triangleq \mathbb{P}^0(P_s(\beta) > x), x \in [0, 1], \tag{20}$$

where $\mathbb{P}^0$ is the palm measure (conditioning on the receiver at the origin 0 and on the corresponding transmitter to be active). Since all point processes in the model are ergodic, the meta distribution can be interpreted as the fraction of the active links whose conditional success probabilities are greater than x.

We denote the b-th moment of P_s by M_b, i.e., $M_b \triangleq \mathbb{E}^0(P_s^b)$. In this paper, the beta approximation method is selected to derive the meta distribution [20], which requires only the first and second moments. Accordingly, the b-th moment of $P_s(\beta)$ is given by [22]

$$M_b(\beta) \triangleq \mathbb{E}\left[P_s(\beta)^b\right] = \int_0^1 \mathrm{b}x^{b-1}\bar{F}_{P_s}(x)\mathrm{d}x, b \in \mathbb{Z}. \tag{21}$$

Some important performance characteristics are acquired through Equation (21). They include $p_s(\beta) \equiv M_1(\beta)$, the variance $M_2 - M_1^2$ of $P_s(\beta)$, and the mean local delay M_{-1} from the -1-st moment of $P_c(\beta)$.

For the typical CU, the b-th moment of the conditional success probability is

$$M_{b,\mathrm{cu}} = \frac{\pi\lambda_b}{A_1}\int_D^{\infty} e^{-\lambda_b r_c(\pi-(\Psi/2)+C(\beta,b))}\mathrm{d}r_c, b \in \mathbb{Z}, \tag{22}$$

where $C(\beta, b) = \int_0^{\Psi/2} {}_2F_1[-(2/\alpha), b, 1-(2/\alpha), -\beta e^{-\theta}]d\theta$, and ${}_2F_1[a, b; c; z]$ is the Gaussian hyper-geometric function.

Proof. See Appendix C.

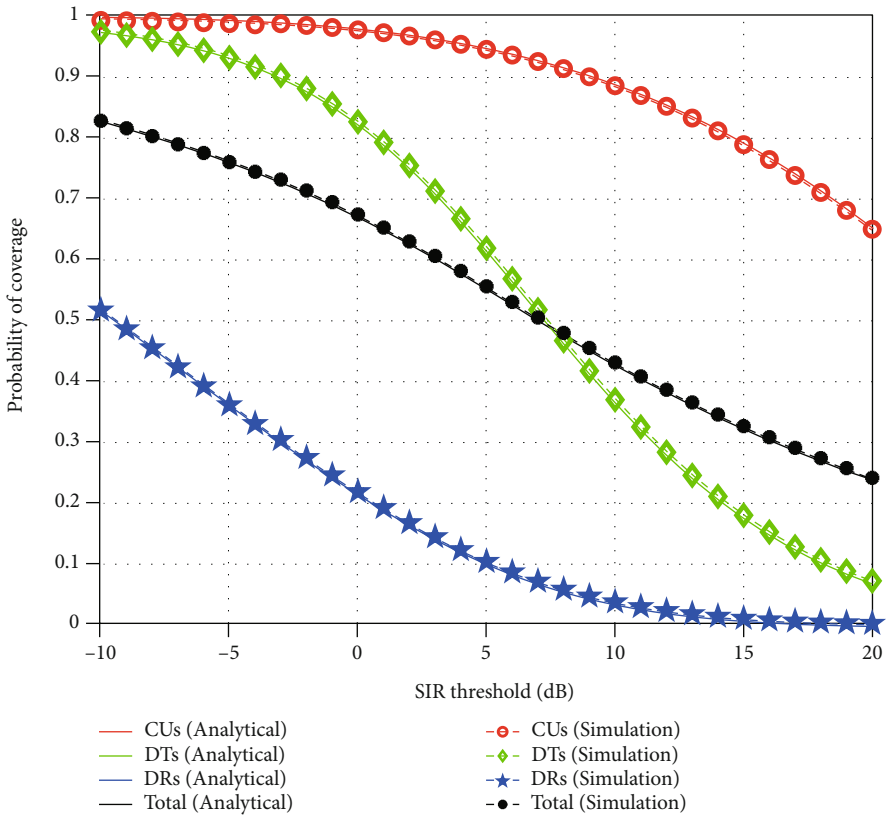

(a) $t_1/t_2 = 1$

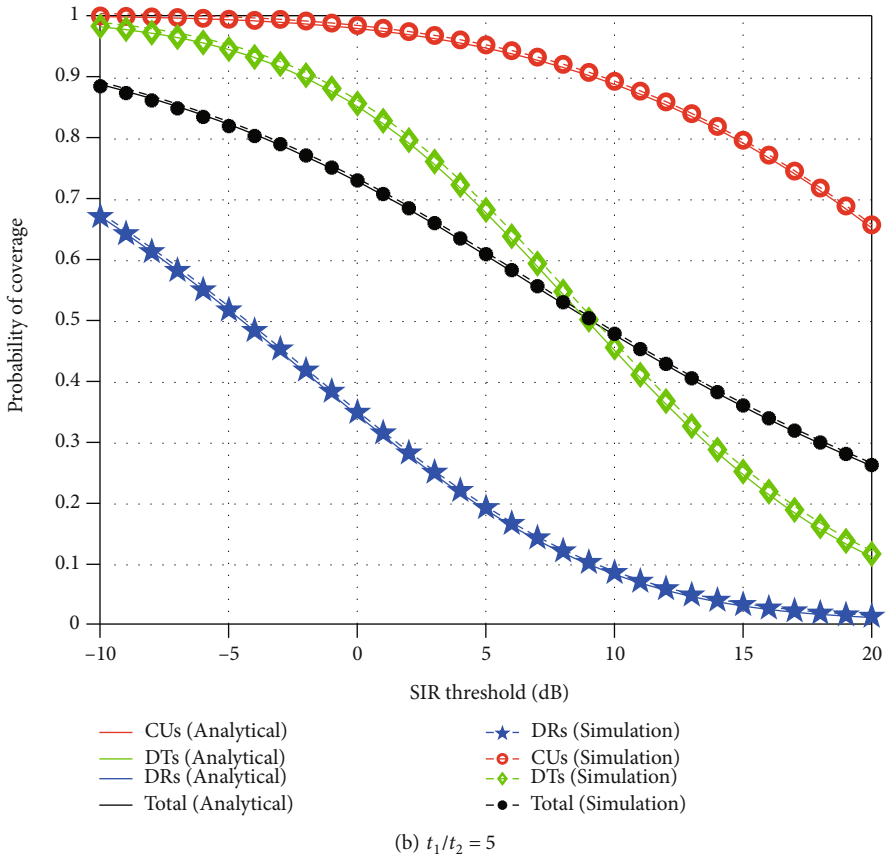

(b) $t_1/t_2 = 5$

FIGURE 3: The mean M_1 of the conditional success probability under the proposed D2D network model.

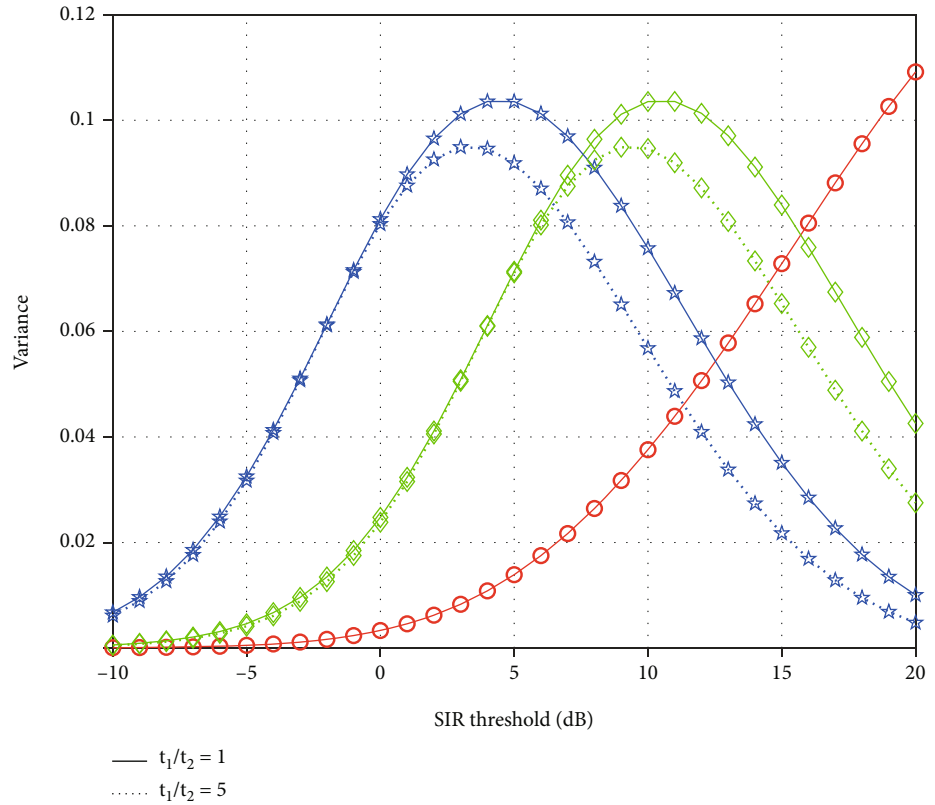

FIGURE 4: The comparison of the variance depends on the SIR threshold values and the ratio of t_1 to t_2.

For the typical DT, the b-th moment of the conditional success probability is

$$M_{b,\mathrm{dt}} = \frac{\pi\lambda_b}{A_2}\int_D e^{-(t_1/t_1+t_2)\lambda_b r_d(\pi-(\Psi/2)+C_1(\beta,b))} e^{-(t_2/t_1+t_2)(P_u/P_b)2\pi\lambda_d r_d C_2(T,b)}\mathrm{d}r_d,\ b\in\mathbb{Z}. \tag{23}$$

Similarly, for the typical DR, the b-th moment of the conditional success probability is

$$M_{b,\mathrm{dr}} = \frac{8\pi^3\lambda_d\lambda_b^2}{A_2^2}\int_D\int_0^\infty e^{-(t_1/t_1+t_2)(P_b/P_u)\lambda_d r_d^2 y(\pi-(\Psi/2)+C_1(\beta,b))} e^{-(t_2/t_1+t_2)2\pi\lambda_d y C_2(T,b)}\mathrm{d}y\mathrm{d}r_d,\ b\in\mathbb{Z}, \tag{24}$$

where $C_1(\beta,b)=\int_0^{\Psi/2}{}_2F_1[-(2/\alpha),b,1-(2/\alpha),-\beta e^{-\theta}]d\theta$ and $C_2(T,b)={}_2F_1[-(2/\alpha),b,1-(2/\alpha),-T]$.

Theorem 3. (Meta Distribution of the Whole Network). *For the overall users, the meta distribution of the SIR is*

$$M_{b,total} = A_1 M_{b,cu} + A_2 M_{b,dt} + A_2 M_{b,dr},\ b\in\mathbb{Z}, \tag{25}$$

where the $M_{b,cu}$, $M_{b,dt}$, and $M_{b,dr}$ are given by Equations (22), (23), and (24), respectively.

4.5. The Mean Local Delay. Generally, the per link delay consists of four types of delays, namely, the processing delay, the queueing delay, the transmission delay, and the propagation delay. In most wireless networks, the processing delay and the propagation delay are negligible compared to the queueing delay and the transmission delay. The main component of the transmission delay is the retransmission delay which is closely related to the number of retransmissions of a packet. This type of delay is often called local delay. The mean local delay is defined as the mean number of transmissions until the first success [20]. It is finite when certain parameters of the network, such as the SIR threshold and the medium access probability, are below specific thresholds. From (21), the mean local delay for the typical CU is given by:

$$M_{-1,\mathrm{cu}} = \frac{\pi\lambda_b}{A_1}\int_D^\infty e^{-\lambda_b r_c(\pi-(\Psi/2)+C(\beta))}\mathrm{d}r_c, \tag{26}$$

where $C(\beta)=\int_0^{\Psi/2}{}_2F_1[-(2/\alpha),-1,1-(2/\alpha),-\beta e^{-\theta}]d\theta$.

From (23), the mean local delay for the typical DT is given by

$$M_{-1,\mathrm{dt}} = \frac{\pi\lambda_b}{A_2}\int_D^\infty e^{-(t_1/t_1+t_2)\lambda_b r_d(\pi-(\Psi/2)+C_1(\beta))} e^{-(t_2/t_1+t_2)(P_u/P_b)2\pi\lambda_d r_d C_2(T)}\mathrm{d}r_d. \tag{27}$$

From (24), the mean local delay for the typical DR is given by

$$M_{-1,\mathrm{dr}} = \frac{8\pi^3\lambda_d\lambda_b^2}{A_2^2}\int_D\int_0^\infty e^{-(t_1/t_1+t_2)(P_b/P_u)\lambda_d r_d^2 y(\pi-(\Psi/2)+C_1(\beta))} e^{-(t_2/t_1+t_2)2\pi\lambda_d y C_2(T)}\mathrm{d}y\mathrm{d}r_d, \tag{28}$$

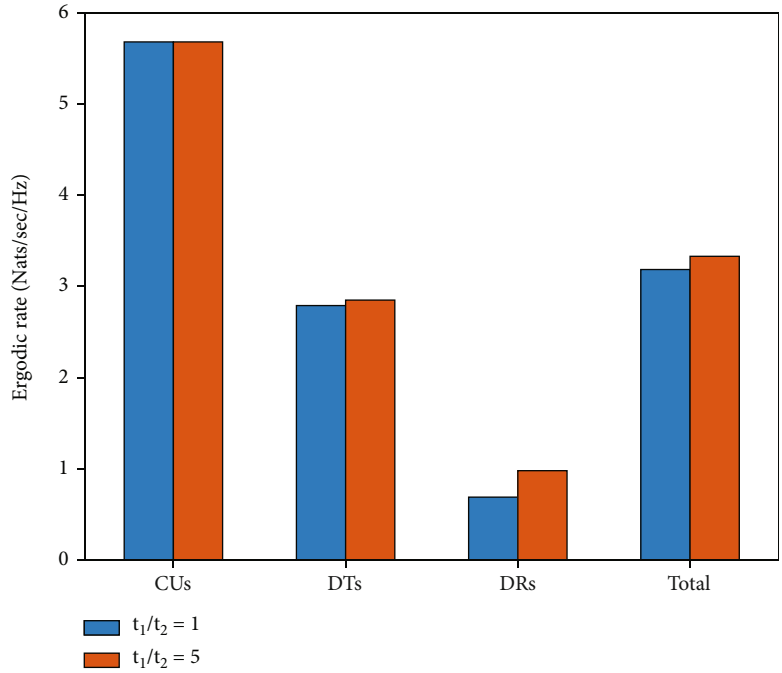

Figure 5: The comparison of the ergodic transmission rate for the proposed D2D network.

where $C_1(\beta) = \int_0^{\Psi/2} {}_2F_1[-(2/\alpha),-1, 1-(2/\alpha),-\beta e^{-\theta}]d\theta$ and $C_2(T) = {}_2F_1[-(2/\alpha),-1, 1-(2/\alpha),-T]$.

5. Numerical Results

This section validates the correctness of the proposed D2D relaying scheme through MATLAB Monte-Carlo method. The simulation environment is built according to the system model in Section 2. And the following parameters are set according to the LTE-A.

Specifically, the network area is 1000m × 1000m, BSs are placed in the establishment area according to PPP with $\lambda_b = 20$SBSs/km^2, and users are placed with $\lambda_u = 800$users/km^2. We consider the SIR threshold for cellular links, and D2D links β and T have the same change. The path loss exponent is $\alpha = 4$. To improve the quality of cell coverage, the angle of directional antennas Ψ is set to $\pi/2$. The reliability of simulation results is based on the statistical average of 20,000 snapshots, so it can more accurately reflect the performance of users in the proposed D2D network. Table 2 summarizes the simulation parameters.

The coverage probabilities as a function of SIR threshold are presented in Figure 3 for the proposed D2D network. Figures 3(a) and 3(b) compare coverage probabilities of different types of users under different time slot divisions. Our analysis concretely demonstrates that the coverage probability always decreases when higher SIR threshold in Figures 3(a) and 3(b). This is because the interference suffered by users increased with higher SIR threshold, resulting that fewer users can successfully connect to the network. Through two figures, the intuition behind this observation is that the ratio of t_1 to t_2 does not affect CUs because CUs are always connected to their serving BSs. For DUs, it can be seen that the coverage probability of D2D receivers increases significantly with the ratio of t_1 to t_2 increases, while it has little impact on D2D transmitters. This is because the larger the proportion of t_1, the more DTs that can successfully communicate with BSs in t_1 stage. Therefore, more DTs can successfully forward data from BSs in t_2 stage, and the number of successful D2D links increases accordingly. However, the interference received by DTs from the BSs (except their serving BS) also increases as the proportion of t_1 phase increases, but the coverage probability of DTs is still improved slightly. Therefore, the time slot ratio of cellular link is proportional to the total coverage probability of network.

The variance of different types of users as a function of SIR threshold for different ratios of t_1 to t_2 is plotted in Figure 4, where the red, green, and blue lines represent CUs, DTs, and DRs, respectively. Hence, the values of SIR for the great majority of users are difficult to meet threshold value for DUs, especially in the high threshold value, leading to a relatively quick decline of the variance line. Furthermore, the variance of DUs is smaller when $t_1/t_2 = 5$. Interestingly enough, the decrease does not occur, and the increasing trend of variance continues for the BS-CU link. This hints that the communication service quality of all users becomes robust as the distance decreases between BS to user.

In Figure 5, the comparison results of the ergodic transmission rate with units nats/Hz (1 bit = ln (2) = 0.693 nats) for different types of users are plotted by the bar graph. The blue bar and orange bar graphs represent different times s1ot ratios, respectively. As shown in Figure 4, the total ergodic transmission rate increases with the ratio of t_1 to t_2 in the considered range. The reason is the same as the analysis of coverage probability.

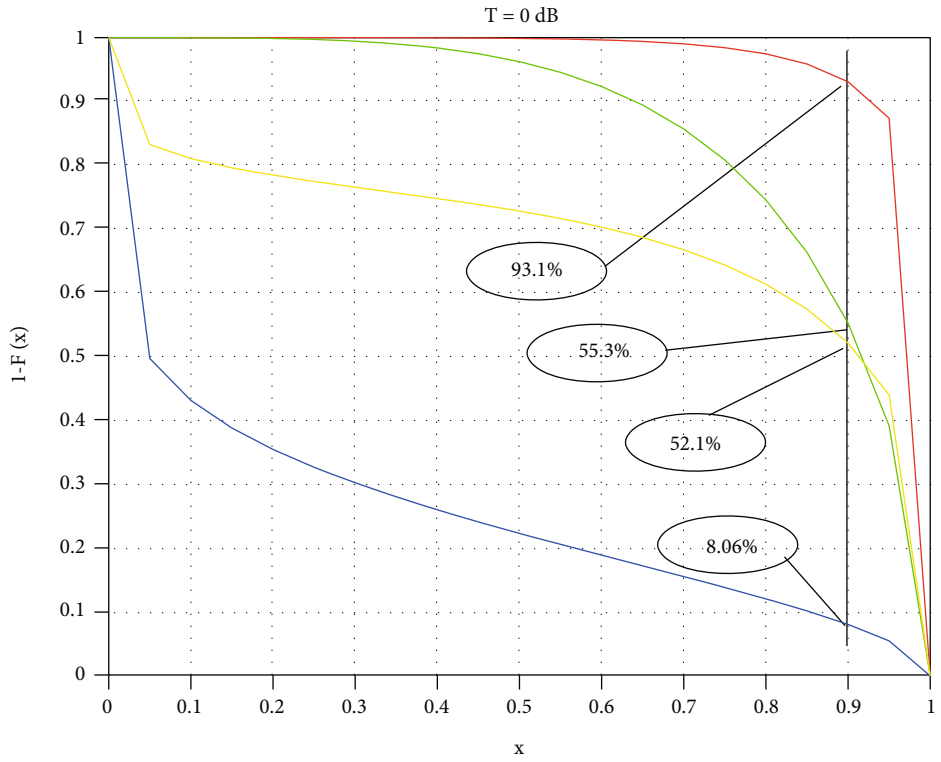

(a) $T = 0$ dB

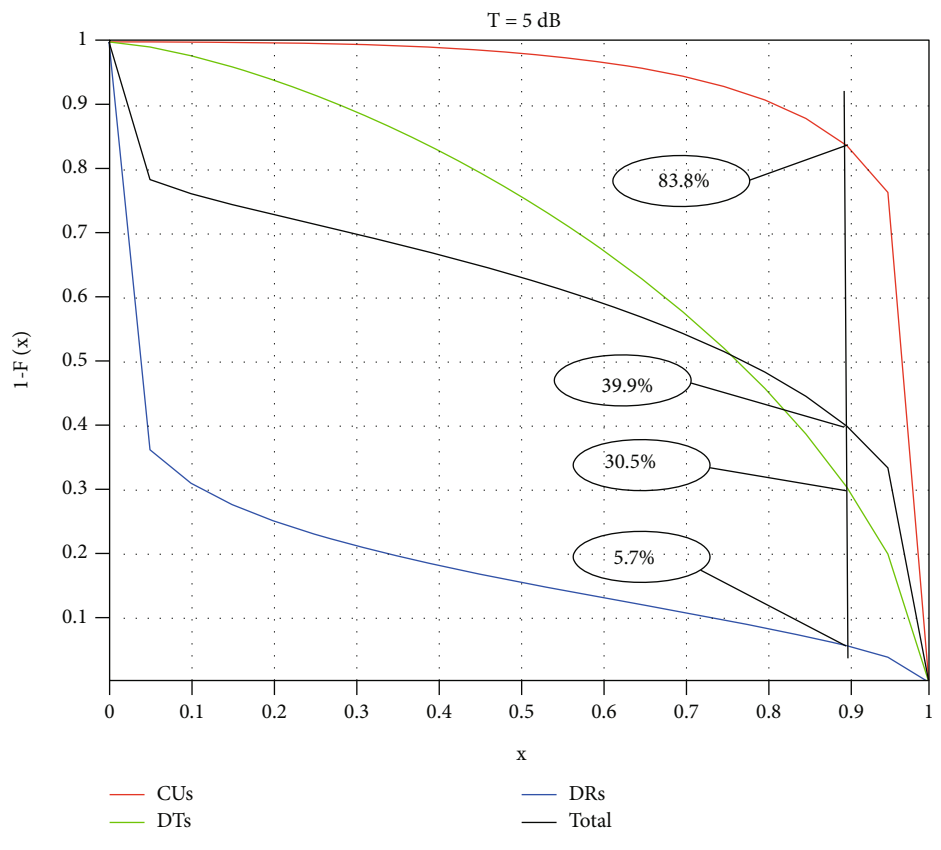

(b) $T = 5$ dB

Figure 6: The meta distribution of SIR for D2D networks when the value of SIR threshold is fixed, where the ratio of t_1 to t_2 is 5.

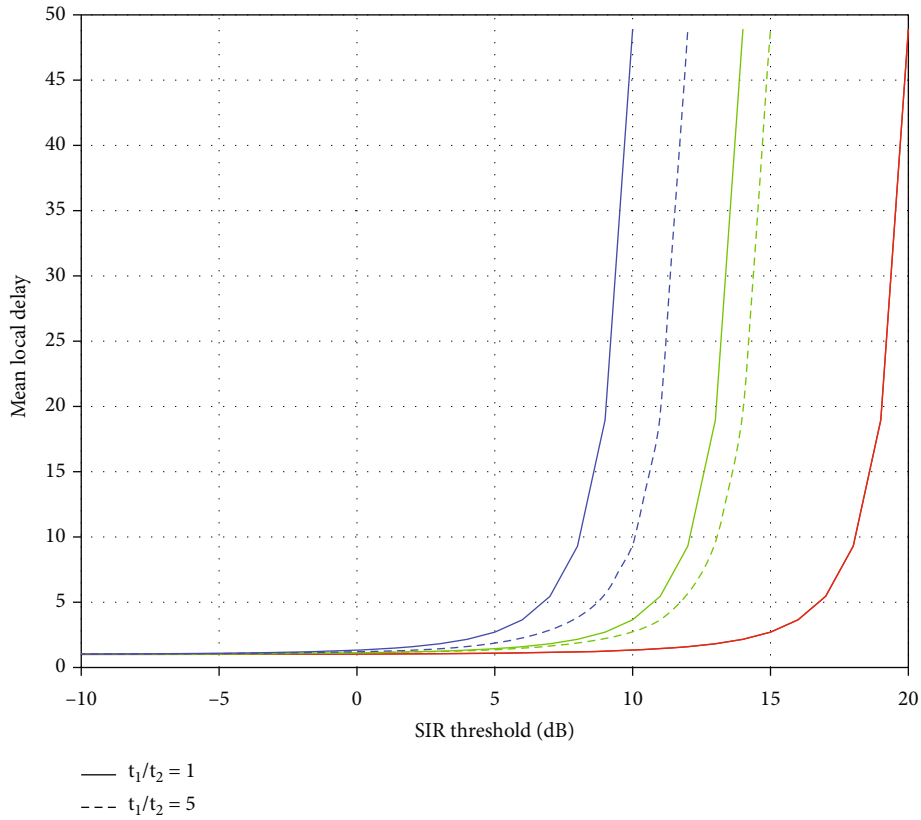

Figure 7: The mean local delay of different types of users under the proposed D2D network model.

When SIR threshold is fixed, the meta distributions of SIR with different values of given coverage probability x are investigated in Figure 6. The number of users whose conditional success probabilities meet a given value of x increases as the ratio of t_1 to t_2, so we choose the case of $t_1/t_2 = 5$ to analyze. In Figure 6(a), when $T = 0$ dB, the proportion of CUs, DTs, and DRs who achieve the successful communication probability exceeding 0.9 are 93.1%, 56.3%, and 8.06%, respectively. Therefore, the proportion of the whole network users achieve the successful communication probability exceeding 0.9 is 52.1%. When $T = 5$ dB, the communication link qualities of all users are stronger than that of $T = 0$ dB in the D2D network. Consequently, in Figure 6(b), the proportion of CUs, DTs, and DRs who exceed the same value of x are drop to 83.8%, 30.5%, and 5.7%, respectively, and the whole network is 39.9%.

In Figure 7, the mean local delay of users is illustrated as a function of SIR threshold for different ratios of t_1 to t_2, where the red, green, and blue lines represent CUs, DTs, and DRs, respectively. The mean local delay is the mean number of transmission attempts needed to succeed once if the transmitter is allowed to keep transmitting until success. As ratio of t_1 to t_2 approaches equality, this means that a significant fraction of D2D links suffers from high delay, which is certainly an undesirable operating regime. This is because success probability of DRs decreases in the time slot t_2 with the number of successful DTs in t_1. It is also notable that the mean local delay rushes to infinity when some certain SIR thresholds are reached for all users.

6. Conclusions

In this paper, we developed a comprehensive framework for the performance analysis of D2D networks with a distance-based D2D relaying mechanism, which is suitable for edge users because it allows a reduction of the distance with their serving source. The key idea of our policy is that the BS selects a user outside a disk of predefined radius D around BS as a relay in the first time slot and the relay user forwards the information received by BS in the next slot for D2D communication. Since different time slots have different transmission sources, we model a nonsynchronization system realistically, so interference caused by BS for DUs is considered. We developed a tractable approach to model the locations of users and BSs as PPP. In particular, we assumed the overlay in-band D2D, so the DUs can be modeled as PHP approximately due to the orthogonal spectrum of CUs and DUs. For this setup, we derive analytical expressions for the coverage probability, the average transmission rate of different types of users, and the whole network using stochastic geometry, which takes the allocation of time resources into account. As a key intermediate step, we characterized the distributions of the cochannel interference and cross-tier interference for DUs. Furthermore, the meta distribution of SIR and mean local delay in the proposed D2D network were derived for both cellular and D2D users. For numerical evaluation, we discovered that more time consumed by BS-DT links has the same effect on the BS-DT links and DT-DR links in terms of coverage and

transmission rate; i.e., both of these two performance indicators for these links will be favored. Thus, the number of users who can successfully access to the network also has improved. This observation shows that more D2D links can be successfully established with more DTs who successfully communicate.

An extension of this work is to optimize some performance indicators such as energy efficiency and spectrum efficiency of D2D networks. Further, this work can be extended to the scenario where the D2D users can be in different cells in a distributed approach. In this scenario, the relay would have to act as a BS.

Appendix

A. Proof of Equation (8)

Combined with the distribution of R_c, the average successful communication probability of the typical CU is expressed as

$$\begin{aligned}
\mathrm{P}_c^{\mathrm{cu}} &= \int_0^D \mathbb{P}(\mathrm{SIR} > \beta | r_c) f_{R_c}(r_c|D) dr_c \\
&= \int_0^D \mathbb{P}\left(\frac{P_b h r_c^{-\alpha}}{\sum_{i\in\Phi_b\setminus\{b_o\}} P_b h_i R_i^{-\alpha}} > \beta | r_c \right) f_{R_c}(r_c|D) dr_c \\
&= \int_0^D \mathbb{P}\left(h > \frac{\beta r_c^{\alpha} \sum_{i\in\Phi_b\setminus\{b_o\}} P_b h_i R_i^{-\alpha}}{P_b} | r_c \right) f_{R_c}(r_c|D) dr_c \\
&\overset{(a)}{=} \int_0^D \exp\left(-\beta r_c^{\alpha} \sum_{i\in\Phi_b\setminus\{b_o\}} P_b h_i R_i^{-\alpha} \right) f_{R_c}(r_c|D) dr_c \\
&\overset{(b)}{=} \int_0^D \mathscr{L}_{I_c}(\beta r_c^{\alpha}) f_{R_c}(r_c|D) dr_c,
\end{aligned} \tag{A.1}$$

where $f_{R_c}(r_c|D)$ are given by Equation (4), (a) follows from $h \sim \exp(1)$, and $\mathscr{L}_{I_c}(\beta r_c^{\alpha})$ is the *Laplace* transform of cumulative interference function I_c, $\mathscr{L}_{I_c}(\beta r_c^{\alpha}) = \mathbb{E}[e^{-\beta r_c^{\alpha} I_c}]$.

Therefore,

$$\begin{aligned}
\mathscr{L}(\beta r_c^{\alpha}) &= \mathbb{E}_{R,h,\theta}\left[\prod_{i\in\Phi_b\setminus\{b_o\}} e^{-\beta r_c^{\alpha} h R^{-\alpha} e^{-|\theta|}} \right] = \mathbb{E}_{R,\theta}\left[\prod_{i\in\Phi_b\setminus\{b_o\}} \frac{1}{1+\beta r_c^{\alpha} R^{-\alpha} e^{-|\theta|}} \right] \\
&\overset{(a)}{=} \mathbb{E}_R\left[\prod_{i\in\Phi_b\setminus\{b_o\}} \int_{-\Psi/2}^{\Psi/2} \frac{1}{1+\beta r_c^{\alpha} R^{-\alpha} e^{-\theta}} \frac{1}{2\pi} d\theta \right] \\
&\overset{(b)}{=} \exp\left(-2\lambda_b \int_{r_c}^{\infty} \int_0^{\Psi/2} \frac{\nu\beta}{\beta + (\nu/r_c)^{\alpha} e^{\theta}} d\theta \mathrm{d}\nu \right),
\end{aligned} \tag{A.2}$$

where steps (a) are based on the i.i.d. characteristics of $\{h_i\}$ and $\{\theta_i\}$, respectively. Steps (b) is used the probability generating functional (PGFL) of the PPP [36]. Then, let $\nu/r_c = m$,

$$\mathscr{L}(\beta r_c^{\alpha}) = r_c^2 \int_1^{\infty} \int_0^{(\Psi/2)} \frac{m\beta}{\beta + m^{\alpha} e^{\theta}} d\theta \mathrm{d}m. \tag{A.3}$$

From Equations (4), (A.1), and (A.3), Equation (8) is obtained.

B. Proof of Equation (11)

Proof.

$$P_c^{\mathrm{dr}} = \mathbb{P}(\mathrm{SIR}_{\mathrm{dt}} > \beta, \mathrm{SIR}_{\mathrm{dr}} > T) \geq \mathbb{P}(\mathrm{SIR}_{\mathrm{dt}} > \beta)\mathbb{P}(\mathrm{SIR}_{\mathrm{dr}} > T), \tag{A.4}$$

where $\mathbb{P}(\mathrm{SIR}_{\mathrm{dt}} > \beta)$ is given by Equation (9).

$$\begin{aligned}
\mathbb{P}(\mathrm{SIR}_{\mathrm{dr}} > T) &= \int_0^{\infty} \mathbb{P}(\mathrm{SIR} > T | y) f_Y(y) \mathrm{d}r \\
&= \int_0^{\infty} \mathscr{L}_{\mathrm{Ic}}\left(\frac{\beta y^{\alpha}}{P_u} \right) \mathscr{L}_{\mathrm{Id}}(\mathrm{T}y^{\alpha}) f_Y(y) \mathrm{d}y,
\end{aligned} \tag{A.5}$$

where

$$\begin{aligned}
\mathscr{L}_{\mathrm{Ic}}\left(\frac{\beta y^{\alpha}}{P_u} \right) &= e^{-\beta y^{\alpha}(P_b/P_u)(t_1/t_1+t_2) \sum_{i\in\Phi_b\setminus\{b_o\}} h_i R_i^{-\alpha} e^{-|\theta_i|}} \\
&= \int_D^{\infty} \exp\left(-2\lambda_b \int_{r_d}^{\infty} \int_0^{\Psi/2} \frac{1}{1+(t_1+t_2/t_1)(P_u/P_b)\beta(\nu/y)^{-\alpha} e^{\theta}} \mathrm{v}d\theta \mathrm{d}v \right) \\
&\quad \times f_{R_d}(r_d|D) \mathrm{d}r_d,
\end{aligned} \tag{A.6}$$

Similarly, $\mathscr{L}_{\mathrm{Id}}(\mathrm{T}y^{\alpha}) = \exp\left(-2\pi\lambda_d \int_0^{\infty} (\mathrm{v}\mathrm{T}/T + (t_1+t_2/t_2)(\nu/y)^{\alpha}) \mathrm{d}v\right)$. The reason why the integral lower limit starts at 0 is that the interference distance may be smaller than the service distance. Combined with Equations (A.5) and (A.6), the coverage probability of the DT-DR link is given by

$$\mathbb{P}(\mathrm{SIR}_{\mathrm{dr}} > T) = \frac{4\pi^2 \lambda_b \lambda_d}{A_2} \int_0^{\infty} \int_D^{\infty} r_d y \, e^{-\lambda_b \left(\pi r_d^2 + 2F_4(r_d,\beta) + 2\pi y^2 e^{-\lambda_b \pi D^2} F_5(T) \right) - \lambda_d \pi y^2} \mathrm{d}r_d \mathrm{d}y. \tag{A.7}$$

Therefore, combined with Equations (6), (9), and (A.4), Equation (11) is obtained.

C. Proof of Equation (22)

Proof.

$$P_{c,\mathrm{cu}}(\beta) = \mathbb{P}[\mathrm{SIR}_c > \beta | \Phi_s] = \prod_{i\in\Phi_b\setminus b_o} \frac{1}{1 + T r_c^{\alpha} R_i^{-\alpha} \left(1/e^{|\theta_i|} \right)}. \tag{A.8}$$

According to Equation (21), $M_{b,\mathrm{cu}}$ is given by

$$\begin{aligned} M_{b,\mathrm{cu}} &= \mathbb{E}_{r_c}\left[\mathbb{E}_{R_i}\prod_{i\in\Phi_b\setminus b_o}\mathbb{E}_{\theta_i}\left[\frac{1}{\left(1+\beta r_c^{\alpha}R_i^{-\alpha}\left(1/e^{|\theta_i|}\right)\right)^{b}}\right]\right] \\ &= \exp\left(-2\lambda_b\int_{r_c}^{\infty}\left(\int_0^{\Psi/2}\left[1-\frac{1}{\left(1+\beta r_c^{\alpha}v^{-\alpha}\left(1/e^{\theta}\right)\right)^{b}}\right]d\theta\right)\mathrm{vdv}\right) \\ &= \exp\left(-\lambda_b\beta^{2/\alpha}r_c^2\int_0^{\Psi/2}\left(\frac{1}{e^{\theta}}\right)^{2/\alpha}F_2\left(\beta^{-2/\alpha}\left(\frac{1}{e^{\theta}}\right)^{-2/\alpha}\right)d\theta\right). \end{aligned} \tag{A.9}$$

Let $g = T^{-2/\alpha}\left(1/e^{\theta}\right)^{-2/\alpha}$, $F_2(g)$ of Equation (A.9) can be expressed as follows by the *Gaussian* hyper-geometric function

$$F_2(g) = \int_g^{\infty}\left(1-\frac{1}{\left(1+u^{-\alpha/2}\right)^{b}}\right)\mathrm{du} = g\left(-1+{}_2F_1\left(-\frac{\alpha}{2},b,1-\frac{\alpha}{2},-g^{-\alpha/2}\right)\right). \tag{A.10}$$

Combining Equation (A.8), Equation (22) is proofed.

Data Availability

The data supporting this study are from previously reported studies and datasets, which have been cited. The processed data are available from the corresponding author upon request.

Conflicts of Interest

The authors declare that there is no conflict of interest regarding the publication of this paper.

Acknowledgments

This work was supported by the National Natural Science Foundation of China (NSFC) (61901071), in part by the general project of the Natural Science Foundation of Chongqing (cstc2020jcyj-zdxmX0024).

References

[1] T. Islam, C. Kwon, and Y. Noh, "Transmission power control and relay strategy for increasing access rate in device to device communication," *IEEE Access*, vol. 10, pp. 49975–49990, 2022.

[2] G. Fodor, E. Dahlman, G. Mildh et al., "Design aspects of network assisted device-to-device communications," *IEEE Communications Magazine*, vol. 50, no. 3, pp. 170–177, 2012.

[3] A. Asadi, Q. Wang, and V. Mancuso, "A survey on device-to-device communication in cellular networks," *IEEE Communications Surveys Tutorials*, vol. 16, no. 4, pp. 1801–1819, 2014.

[4] K. Shamganth and M. J. Sibley, "A survey on relay selection in cooperative device-to-device (d2d) communication for 5g cellular networks," in *2017 International Conference on Energy, Communication, Data Analytics and Soft Computing (ICECDS)*, pp. 42–46, 2017.

[5] M. Hasan, E. Hossain, and D. I. Kim, "Resource allocation under channel uncertainties for relay-aided device-to-device communication underlaying lte-a cellular networks," *IEEE Transactions on Wireless Communications*, vol. 13, no. 4, pp. 2322–2338, 2014.

[6] M. Naslcheraghi, L. Marandi, and S. A. Ghorashi, "A novel device-to-device discovery scheme for underlay cellular networks," in *2017 Iranian Conference on Electrical Engineering (ICEE)*, pp. 2106–2110, 2017.

[7] D. D. Ningombam and S. Shin, "Distance-Constrained outage probability analysis for device-to-device communications underlaying cellular networks with frequency reuse factor of 2," *Computers*, vol. 7, no. 4, p. 50, 2018.

[8] D. Ningombam and S. Shin, "Optimal resource management and binary power control in network-assisted d2d communications for higher frequency reuse factor," *Sensors*, vol. 19, no. 2, p. 251, 2019.

[9] D. D. Ningombam and S. Shin, "Traffic offloading in multicast device-to-device cellular networks: a combinatorial auction-based matching algorithm," *Sensors*, vol. 20, no. 4, p. 1128, 2020.

[10] F. Wang and V. K. N. Lau, "Multi-level over-the-air aggregation of mobile edge computing over d2d wireless networks," *IEEE Transactions on Wireless Communications*, pp. 1–1, 2022.

[11] J. Huang, Y. Yang, Z. Gao, D. He, and D. W. K. Ng, "Dynamic spectrum access for d2d-enabled internet-of-things: a deep reinforcement learning approach," *IEEE Internet of Things Journal*, pp. 1–1, 2022.

[12] V. Shah, N. B. Mehta, and R. Yim, "The relay selection and transmission trade-off in cooperative communication systems," *IEEE Transactions on Wireless Communications*, vol. 9, no. 8, pp. 2505–2515, 2010.

[13] M. Seyfi, S. Muhaidat, J. Liang, and M. Dianati, "Effect of feedback delay on the performance of cooperative networks with relay selection," *IEEE Transactions on Wireless Communications*, vol. 10, no. 12, pp. 4161–4171, 2011.

[14] K. O. Odeyemi and P. A. Owolawi, "Performance analysis of cooperative noma with partial relay selection under outdated channel estimate," in *2019 IEEE 2nd Wireless Africa Conference (WAC)*, pp. 1–5, 2019.

[15] Z. Zhou, S. Zhou, J.-H. Cui, and S. Cui, "Energy-efficient cooperative communication based on power control and selective single-relay in wireless sensor networks," *IEEE Transactions on Wireless Communications*, vol. 7, no. 8, pp. 3066–3078, 2008.

[16] A. Bletsas, H. Shin, and M. Z. Win, "Cooperative communications with outage-optimal opportunistic relaying," *IEEE Transactions on Wireless Communications*, vol. 6, no. 9, pp. 3450–3460, 2007.

[17] X. Lin, J. G. Andrews, and A. Ghosh, "Spectrum sharing for device-to-device communication in cellular networks," *IEEE Transactions on Wireless Communications*, vol. 13, no. 12, pp. 6727–6740, 2014.

[18] G. George, R. K. Mungara, and A. Lozano, "An analytical framework for device-to-device communication in cellular networks," *IEEE Transactions on Wireless Communications*, vol. 14, no. 11, pp. 6297–6310, 2015.

[19] A. H. Sakr and E. Hossain, "Cognitive and energy harvesting-based d2d communication in cellular networks: stochastic geometry modeling and analysis," *IEEE Transactions on Communications*, vol. 63, no. 5, pp. 1867–1880, 2015.

[20] M. Haenggi, "The meta distribution of the sir in poisson bipolar and cellular networks," *IEEE Transactions on Wireless Communications*, vol. 15, no. 4, pp. 2577–2589, 2016.

[21] L. Yang, F.-C. Zheng, Y. Zhong, S. Jin, and A. G. Burr, "On the sir meta distribution for cache-enabled wireless networks with random discontinuous transmission: analysis and optimization," *IEEE Transactions on Wireless Communications*, p. 1, 2022.

[22] Q. Liu, J. Zou, and Y. Gu, "Coverage and meta distribution analysis in ultra-dense cellular networks with directional antennas," *IEEE Transactions on Vehicular Technology*, p. 1, 2022.

[23] L. Yang, F.-C. Zheng, Y. Zhong, and S. Jin, "Spatio-Temporal analysis of meta distribution for cell-center/cell-edge users," *IEEE Transactions on Communications*, vol. 69, no. 12, pp. 8256–8270, 2021.

[24] M. Salehi, A. Mohammadi, and M. Haenggi, "Analysis of d2d underlaid cellular networks: sir meta distribution and mean local delay," *IEEE Transactions on Communications*, vol. 65, no. 7, pp. 2904–2916, 2017.

[25] M. Afshang, H. S. Dhillon, and P. H. Joo Chong, "Modeling and performance analysis of clustered device-to-device networks," *IEEE Transactions on Wireless Communications*, vol. 15, no. 7, pp. 4957–4972, 2016.

[26] F. Tong, Y. Wan, L. Zheng, J. Pan, and L. Cai, "A probabilistic distance-based modeling and analysis for cellular networks with underlaying device-to-device communications," *IEEE Transactions on Wireless Communications*, vol. 16, no. 1, pp. 451–463, 2017.

[27] A. Abdallah, M. M. Mansour, and A. Chehab, "Power control and channel allocation for d2d underlaid cellular networks," *IEEE Transactions on Communications*, vol. 66, no. 7, pp. 3217–3234, 2018.

[28] D. Jaswanth, S. K. Sahoo, G. Satapathy, and S. P. Dash, "Optimal coverage analysis of a cp-ofdm/fbmc based device-to-device communication system," in *2021 IEEE 93rd Vehicular Technology Conference (VTC2021-Spring)*, pp. 1–6, 2021.

[29] M. Chu, A. Liu, J. Chen, V. K. N. Lau, and S. Cui, "A stochastic geometry analysis for energy-harvesting-based device-to-device communication," *IEEE Internet of Things Journal*, vol. 9, no. 2, pp. 1591–1607, 2022.

[30] S. Badri and M. Rasti, "Interference management and duplex mode selection in in-band full duplex d2d communications: a stochastic geometry approach," *IEEE Transactions on Mobile Computing*, vol. 20, no. 6, pp. 2212–2223, 2021.

[31] Y. Ye, S. Huang, M. Xiao, Z. Ma, and M. Skoglund, "Cache-enabled millimeter wave cellular networks with clusters," *IEEE Transactions on Communications*, vol. 68, no. 12, pp. 7732–7745, 2020.

[32] P. D. Mankar, Z. Chen, M. A. Abd-Elmagid, N. Pappas, and H. S. Dhillon, "Throughput and age of information in a cellular-based iot network," *IEEE Transactions on Wireless Communications*, vol. 20, no. 12, pp. 8248–8263, 2021.

[33] C. V. Anamuro, N. Varsier, J. Schwoerer, and X. Lagrange, "Distance-aware relay selection in an energy-efficient discovery protocol for 5g d2d communication," *IEEE Transactions on Wireless Communications*, vol. 20, no. 7, pp. 4379–4391, 2021.

[34] Z. Yazdanshenasan, H. S. Dhillon, M. Afshang, and P. H. J. Chong, "Poisson hole process: theory and applications to wireless networks," *IEEE Transactions on Wireless Communications*, vol. 15, no. 11, pp. 7531–7546, 2016.

[35] M. Ding and D. López-Pérez, "On the performance of practical ultra-dense networks: the major and minor factors," in *Proc. IEEE Workshop Spatial Stochastic Models Wireless Netw. (SpaSWiN)*, pp. 1–8, Paris, France, 2017.

[36] J. G. Andrews, F. Baccelli, and R. K. Ganti, "A tractable approach to coverage and rate in cellular networks," *IEEE Transactions on Communications*, vol. 59, no. 11, pp. 3122–3134, 2011.

[37] J. G. Andrews, A. K. Gupta, and H. S. Dhillon, "A primer on cellular network analysis using stochastic geometry," 2016, http://arxiv.org/abs/1604.03183.